Targeted Penetration of MCF-7 Cells using Iron-Oxide Nanoparticles In Vitro

Conference Paper · July 2016

DOI: 10.1109/BIOROB.2016.7523635

7 authors, including:

Mahmoud Elfar
Duke University
14 PUBLICATIONS **78** CITATIONS
SEE PROFILE

Mariam Yasser Ayoub
The German University in Cairo
2 PUBLICATIONS **6** CITATIONS
SEE PROFILE

Aya Sameh
2 PUBLICATIONS **6** CITATIONS
SEE PROFILE

Hazem Abass
The German University in Cairo
9 PUBLICATIONS **24** CITATIONS
SEE PROFILE

Targeted Penetration of MCF-7 Cells using Iron-Oxide Nanoparticles *In Vitro*

Mahmoud Elfar[†‡], Mariam Ayoub[*‡], Aya Sameh[*], Hazem Abass[*], Reham M. Abdel-Kader[*], Iman Gomaa[*] and Islam S. M. Khalil[*]

***Abstract*— We achieve selective penetration of MCF-7 breast cancer cells using iron-oxide nanoparticles without causing a permanent damage to the membrane and without any effect on the cell morphology. The nanoparticles are controllably pulled towards the cells under the influence of the magnetic field gradients. First, the nanoparticles are fabricated and their magnetic dipole moment is characterized to be 7.8×10^{-8} A.m^2, at magnetic field of 60 mT and mass of 1.80×10^{-9} kg. This characterization is done by measuring the magnetic force exerted on their dipole moment under the influence of controlled magnetic field gradient. Second, a magnetic-based control system is designed and used to achieve selective targeting of the cells under microscopic guidance. We find that the magnetic control achieves immediate uptake of nanoparticles in the MCF-7 cells without incubation for relatively long time, using magnetic force less than 51 nN. In addition, a microforce sensing probe is used to characterize the impendence of the cells to limit the exerted magnetic force during penetration and to avoid causing damage to the membrane. We find that a single cell can overcome penetration force in excess of 13.3 μN.**

I. INTRODUCTION

Selective targeting of cancer cells using magnetic agents [1], [2] has diverse biomedical applications such as targeted therapy [3], [4], diagnosis, penetrating tissues for noninvasive surgeries, and testing of chemotherapeutic agents [5], [6]. The advancement in nano-technology enables fabrication of these magnetic agents at micro- and nano-scales, and hence they can controllably reach deep-seated regions in the human body and achieve non-trivial tasks. The cellular uptake of microparticles has been studied by Gratton *et al.*, and it has been demonstrated that microparticles with high aspect ratios are more prone to cell uptake [7]. Wang *et al.* have demonstrated ultrasonic propulsion of gold nanomotors inside HeLa cervical cancer cells [8]. The acoustic propulsion of these nanomotors allows them to remain active inside the cell and enables motion between cells (internalization of the nanomotors is achieved by incubation with the cells for longer than 24 hours). Calero *et al.* [9] have used superparamagnetic iron-oxide nanoparticles to study the uptake rate and internalization dynamics (incubation time of 72 hours). The long incubation time can be avoided and immediate uptake can be achieved through the control of magnetic agents at a distance using feedback control and dynamic magnetic field. Sanchez *et al.* have demonstrated that self-propelled microjects can target and transport multiple neuronal CAD cells (cathecolaminergic cell line) under the influence of externally controlled magnetic fields [10], [11]. However, the locomotion of these microjets depends on the catalytic decomposition of hydrogen peroxide into water and oxygen, and hence they are not suitable for biomedical applications. Liu *et al.* have developed a robotic adherent cell injection system that enables large-scale cell injection with high success rates [12]. Enikov *et al.* have also quantified the interaction forces during intracytoplasmic injections using a micro-electro-mechanical system that is based on force measurement [13].

In this work, we experimentally demonstrate cell penetration using biocompatible iron-oxide nanoparticles without incubation. The cell uptake is achieved in a few minutes

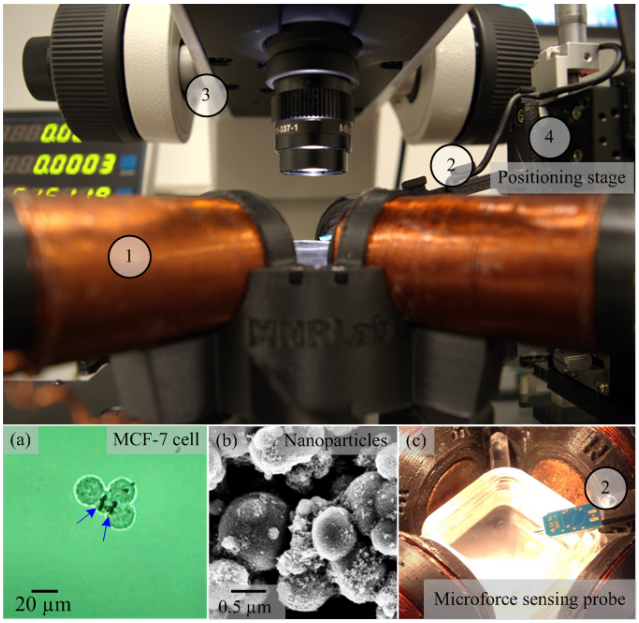

Fig. 1. An electromagnetic system ① with a microforce sensing probe ② for the selective penetration of MCF-7 breast cancer cells (a) using iron-oxide nanoparticles (b). The cells and the nanoparticles are contained inside a reservoir (c) and their positions are determined using a microscopic system ③. The nanoparticles (b) are pulled under the influence of the controlled field gradient towards the cells. The microforce sensing probe (FT-S100 Microforce Sensing Probe, FemtoTools AG, Buchs, Switzerland) is fixed on a 3-axis positioning stage ④ to characterize the penetration force exerted by the nanoparticles on the cells. The post-condition of MCF-7 cell aggregate subjected to penetration with nanoparticles (blue arrows) is shown in inset (a).

This work was supported by funds from the German University in Cairo and the DAAD-BMBF funding project.

[*]The authors are affiliated with the German University in Cairo, New Cairo City 11835, Egypt.

[†]Mahmoud Elfar is affiliated with Duke University, Durham, NC 27708, USA.

[‡]The authors assert equal contribution and joint first authorship.

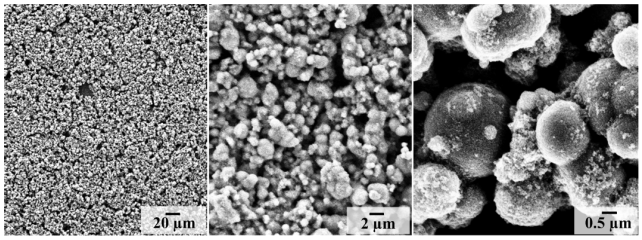

Fig. 2. Scanning Electron Microscopy images of iron oxide nanoparticles. The maximum diameter of the nanoparticles is approximately 2 μm. These nanoparticles are pulled under the influence of the magnetic field gradient towards the MCF-7 cells to achieve immediate uptake. The magnetic dipole moment of a cluster with mass of 1.8×10^{-9} kg is calculated to be 7.8×10^{-8} A.m^2, and the magnetic force exerted on this dipole is measured to be 0.39 μN under the influence of magnetic field gradient of 5 T.m^{-1}. The magnetic field is measured using a 3-axis digital Teslameter (Senis AG, 3MH3A-0.1%-200mT, Neuhofstrasse, Switzerland), and the magnetic field gradients are calculated numerically.

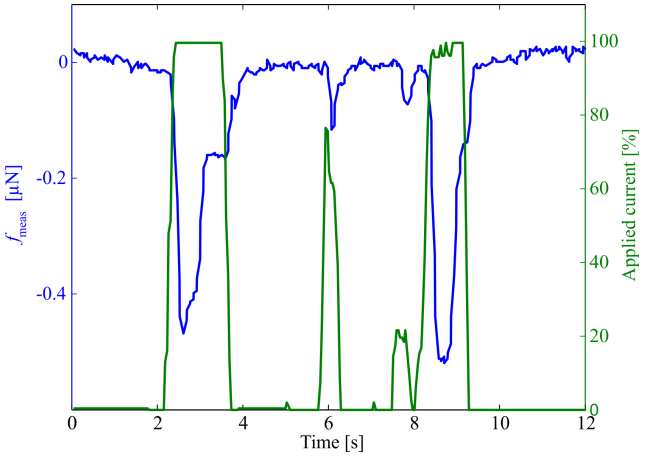

Fig. 3. Interaction forces between the microforce sensing probe (FT-S100 Microforce Sensing Probe, FemtoTools AG, Buchs, Switzerland) and a cluster of iron-oxide nanoparticles. The three peaks represent the interaction forces of a cluster with size of of 5.04×10^5 μm^3. The input current to the electromagnetic coil is increased during the interaction of the cluster with the tip of the microforce sensing probe.

under the influence of the controlled magnetic field gradient exerted on the dipole moment of the nanoparticles [14]. First, we fabricate iron-oxide nanoparticles and characterize the relation between the pulling magnetic force that is exerted on their dipole and the size of the cluster. This characterization is done by using a microforce sensing probe and an electromagnetic system under microscopic guidance (Fig. 1). Second, we culture MCF-7 breast cancer cells and measure the maximum interaction force that does not cause damage to the cell membrane or affect the cell morphology using the microforce sensor probe. We also contain the cells with the nanoparticles to achieve selective penetration and study the accumulation of the nanoparticles inside the cells. The remainder of this paper is organized as follows: Section II provides the fabrication procedures of the iron-oxide nanoparticles, and the characterization of the magnetic force and the magnetic dipole moment. Targeted penetration of the MCF-7 cells is included in Section III. Finally, Section IV concludes and provides directions for future work.

II. FABRICATION, CHARACTERIZATION, AND CONTROL OF IRON-OXIDE NANOPARTICLES

A cluster of iron-oxide nanoparticles is subjected to the following magnetic force ($\mathbf{F}$) and magnetic torque ($\mathbf{T}$) under the influence of external magnetic fields [15], [16]:

$$\mathbf{F} = V\,(\mathbf{m}\cdot\nabla)\,\mathbf{B}(\mathbf{P}) \quad \text{and} \quad \mathbf{T} = V\,(\mathbf{m}\times\mathbf{B}(\mathbf{P}))\,, \qquad (1)$$

where V is the volume of the magnetite nanoparticles. Further, $\mathbf{m}$ and $\mathbf{B}(\mathbf{P})$ are the magnetization (magnetic moment per volume) and the induced magnetic fields at point ($\mathbf{P}$), respectively. We fabricate the iron-oxide nanoparticles, characterize their magnetic properties, and achieve motion control using an electromagnetic system with a microforce sensing probe.

A. Electromagnetic System with Microforce Sensing

Our system consists of an orthogonal array of electromagnetic coils. These coils surround a reservoir that contains the nanoparticles and the MCF-7 cells. The four electromagnetic coils are independently supplied with current inputs using electric drivers (MD10C, Cytron Technologies Sdn. Bhd, Kuala Lumpur, Malaysia) and controlled via an Arduino control board (Arduino MEGA ADK, Arduino, Memphis, Tennessee, U.S.A). The coils provide average magnetic field and field gradient of 55.9 mT and 5 T.m^{-1} (within a workspace of 1.3 mm$\times$1.3 mm), respectively. The positions of the nanoparticles and the cells are tracked using a microscopic system (MF Series 176 Measuring Microscopes, Mitutoyo, Kawasaki, Japan) equipped with a high-speed camera (avA100-120kc, Basler Area Scan Camera, Basler AG, Ahrensburg, Germany) and our feature tracking algorithm [17]. A microforce sensing probe (FT-S100 Microforce Sensing Probe, FemtoTools AG, Buchs, Switzerland) is controlled in three-dimensional space using an automated 3-axis positioning stage. This stage enables accurate positioning of the probe with respect to the cells and the clusters of nanoparticles during the characterization of the interaction forces and magnetic forces, respectively. The positioning stage maintains the orientation of the force sensor such that it has an inclination angle of 15° with the fluid surface. This angle enables the tip of the probe to interact with samples (nanoparticles and cells), while the body of the sensor is kept outside the fluid. A correction factor is applied to the raw measurements provided by the force sensor due to this inclination.

B. Fabrication and Characterization of the Nanoparticles

A mixture of 0.675 g of iron chloride hexahydrate ($FeCl_3\cdot H_2O$), 19 ml of ethylene glycol, 1.8 g of Sodium acetate (NaAc), and 1.0 g of polyethylene glycol is stirred for 30 minutes. The mixture is sealed in a teflon lined stainless-steel autoclave. The autoclave is heated to a temperature of 200°C for 8 hours, and then cooled to room temperature. Finally, the nanoparticles are washed several times with ethanol and dried at 60°C. Fig. 2 provides Scanning Electron Microscopy images of the fabricated iron-oxide nanoparticles. These

nanoparticles are controlled using (1) towards the MCF-7 breast cancer cells.

We characterize the magnetic force exerted on the magnetic dipole moment of the clusters of nanoparticles. This characterization is done using the electromagnetic system and the microforce sensing probe (Fig. 1). The electromagnetic configuration is used to generate a pulling magnetic force to move the cluster of nanoparticles towards the probe. The forces are measured for clusters with size range of 0.5×10^5 μm^3 to 10×10^5 μm^3. First, we inject a controlled amount of nanoparticles into the workspace. The position of the force sensor is controlled such that the sensor tip is in the vicinity of the nanoparticles and at the same work plane. Under microscopic guidance, clusters of nanoparticles are controlled to interact with the tip of the probe. The sensor readings and control inputs to the electromagnetic coils are logged simultaneously in real-time with average sampling rate of 20 sample-per-second. The area of the cluster (in pixels) is estimated using image processing, converted to square micrometers using proper scaling factor, and further multiplied by the average cluster thickness to calculate the measured volume in cubic micrometers. The nanoparticles have spherical morphology (Fig. 2). Therefore, the measured volume is corrected by the following sphere-packing correction factor:

$$V_{\text{eff}} = \frac{\pi}{3\sqrt{2}} V_{\text{meas}}, \tag{2}$$

where V_{eff} and V_{meas} are the effective and measured volumes of the nanoparticles, respectively. The interaction force between a cluster of nanoparticles with volume of 5.04×10^5 μm^3 is shown in Fig. 3. The reading from the ADC chip is converted to micro Newton using the microforce sensing probe gain at which the sensor is calibrated. A correction factor is applied to the measured force as the sensor has an inclination angle of 15° with the surface of the work area, and is given by

$$f_{\text{eff}} = \left(\cos 15 + 0.04 \sin 15\right)^{-1} f_{\text{meas}}, \tag{3}$$

where f_{eff} and f_{meas} are the effective and measured interaction forces, respectively. The difference between the local minimum of the measured force and the idle reading in the vicinity of the local minimum represents the maximum compression force detected by the sensor. The interaction force experiment is repeated 65 times using clusters of sizes that range from 0.5×10^5 μm^3 to 10×10^5 μm^3.

Fig. 4 provides the relationship between volume of the clusters and magnetic forces exerted on their magnetic dipole, under the influence of a magnetic field gradient of 5 T.m^{-1}. The red circles represent the measurements taken during the experiments. These measurements are grouped to 5 representative sizes of clusters of nanoparticles withing the mentioned range (represented by the blue line). The magnetic dipole moment, for a cluster with mass of 1.80×10^{-9} kg and magnetization saturation (M_s) of 55 A.m^2/kg, is calculated to be 9.9×10^{-8} A.m^2. Using the experimental data provided in Fig. 4, the magnetic force exerted on a cluster with mass of 1.80×10^{-9} kg is 0.39 μN, at magnetic field gradient of

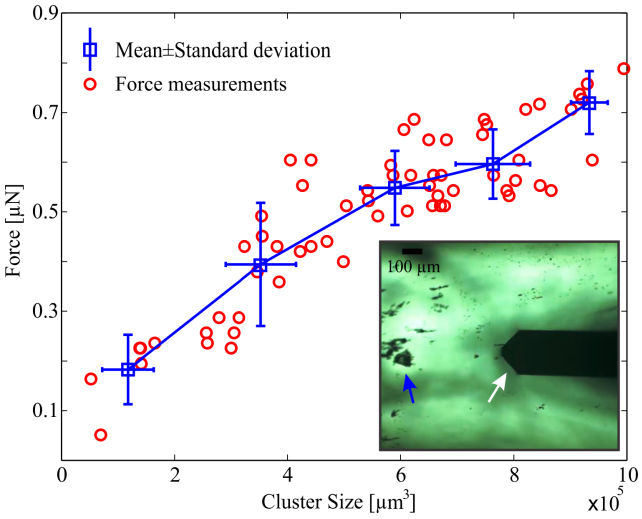

Fig. 4. Interaction force between the microforce sensing probe and clusters of nanoparticles with size range of 0.25×10^6 μm^3 to 3.5×10^6 μm^3. The clusters of nanoparticles are pulled towards the tip of the microforce sensing probe (FT-S100 Microforce Sensing Probe, FemtoTools AG, Buchs, Switzerland) using magnetic field gradient of 5 T.m^{-1}, and the magnetic field is measured to be 60 mT at the tip of the sensor. The magnetic fields are measured using a calibrated 3-axis digital Teslameter (Senis AG, 3MH3A-0.1%-200mT, Neuhofstrasse, Switzerland) and the gradient is calculated numerically. The inset shows a cluster of nanoparticles (blue arrow) and the tip of the microforce sensing probe (white arrow).

5 T.m^{-1}. We use the magnetic force equation (1) and the magnetic dipole moment is calculated to be 7.8×10^{-8} A.m^2. The characterized magnetic dipole is used to design the control system of the cluster of nanoparticles.

C. Magnetic Control of Nanoparticles

The selective penetration of the MCF-7 cells is achieved under magnetic guidance. The magnetic force equation in (1) can be rewritten as follows [18], [19]:

$$\mathbf{F} = V\left(\mathbf{m}\cdot\nabla\right)\tilde{\mathbf{B}}(\mathbf{P})\mathbf{I} = \mathbf{\Lambda}(\mathbf{m},\mathbf{P})\mathbf{I}, \tag{4}$$

where $\tilde{\mathbf{B}}(\mathbf{P})$ and $\mathbf{I}$ are the magnetic field-current map of the electromagnetic system and the input current to the electromagnetic coils, respectively. Further, $\mathbf{\Lambda}(\mathbf{m},\mathbf{P})$ is the magnetic force-current map. This map enables pulling and localization of the cluster of nanoparticles towards and within the vicinity of a reference position, respectively. Fig. 5 provides a representative motion control of a cluster under the influence of the controlled magnetic fields using (4). The cluster is pulled and localized within the vicinity of the reference position (indicated using the small blue circle and the vertical black line), at an average speed of 51.4 μm.s^{-1}. In addition, the magnetic control enables localization with maximum position error of 3.2 μm, in the steady-state. *Please refer to the accompanying video that demonstrates the motion control of a cluster of nanoparticles.*

III. PENETRATION OF CANCER CELLS

We use the electromagnetic system and the iron-oxide nanoparticles to penetrate the MCF-7 breast cancer cells under the influence of the controlled magnetic field gradients [20].

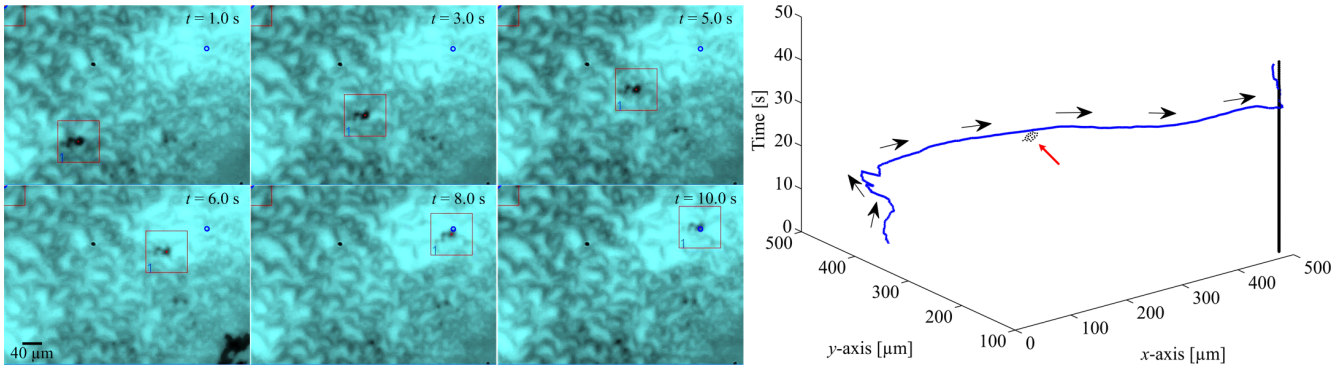

Fig. 5. A representative motion control of a cluster of iron-oxide nanoparticles under the influence of controlled magnetic field gradients. The cluster is pulled towards the reference position (blue small circle) and is localized within its vicinity (vertical black line). The cluster is pulled at an average speed of 51.4 μm.s^{-1}, using magnetic field gradient of 5 T.m^{-1}. The blue line and the black arrows indicate the path of the controlled cluster and its direction, respectively. The red arrow indicate schematically a cluster of nanoparticles. The maximum position error is calculated to be 2 μm and 2.5 μm along x- and y-axis in the steady-state, respectively. *Please refer to the accompanying video that demonstrates the motion control of a cluster of nanoparticles.*

A. Preparation and Characterization of MCF-7 Cells

MCF-7 cells are cultured in RPMI-1640 media (Lonza, 12-702F) containing 10% Fetal Bovine Serum (Lonza, 14-802F) and 1% penicillin-streptomycin (Lonza, 17-602E). The cells are incubated at 5% CO2 and 37°C (Galaxy 170R) until they reach 80-90% confluency. Cells are washed twice using phosphate buffered saline (Lonza, 17-516F), followed by trypsinization (Lonza, CC-5002) and re-suspension in 10 ml of the RPMI-1640 media. The cell suspension is then centrifuged (MIKRO, 22R) at 121xg for 5 minutes at 18°C. The supernatant is aspirated, and the cell pellet is re-suspended in fresh medium. Approximately 0.25×10^6 cells are mounted as cell suspension together with the nanoparticles in a ratio of 1:10 on a microscopic slide for further processing. The average diameter of these cells is calculated to be 20 ± 3 μm.

In order to penetrate the cells without causing damage to the membrane, we apply a compressive force using the tip of controlled microforce sensing probe on the cells. First, the cells are contained inside a channel with width of 2 mm. Second, the 3-axis positioning stage is controlled to push the cell towards the side of the channel to measure the interaction forces, as shown in Fig. 6. In this representative experiment, contact between the probe and the cell is observed at time, t=17.5 seconds. The cell is pushed towards the side of the channel and maximum interaction force of 13.3 μN is measured in this representative experiment. We observe that this interaction force does not cause damage to the cell membrane. This experiment is repeated and we observe consistent results. Therefore, the MCF-7 cells overcome interaction force in excess of 13.3 μN without affecting the cell morphology. The maximum magnetic force exerted on a cluster of nanoparticles with size of 9.9×10^5 μm^3 is measured to be 0.79 μN, as shown in Fig. 4. Therefore, the exerted magnetic force cannot cause damage to the cells during the penetration experiments. *Please refer to the accompanying video that demonstrates the characterization of the MCF-7 cells using the microforce sensing probe.*

B. Penetration of the MCF-7 Breast Cancer Cells

Penetration of the MCF-7 cells is done without incubation of the cells and the nanoparticles. The cells and clusters of nanoparticles are contained within the common center of the electromagnetic configuration. The magnetic field gradient is controlled using (4) to pull the clusters towards the cells. Fig. 7 provides representative trials of the penetration of the MCF-7 breast cancer cells using clusters of nanoparticles. Two clusters with length and width of 10 μm and 4 μm are engulfed by an aggregate of cells after 91 seconds, as shown in Fig. 7 (top). The two clusters are controlled under the influence of magnetic field gradient of approximately 5 T/m. In the second trial (Fig. 7 (bottom)), single cluster with length and width of 6 μm and 4 μm, respectively, is pulled towards single MCF-7 cell and is engulfed after 22 seconds. The pre- and post-conditions of the cells indicate that the nanoparticles uptake is achieved without causing any damage to the cell membrane and without affecting the cell morphology. Fig. 8 provides another representative penetration of an MCF-7 cell using a cluster with width and length of 4 μm and 10 μm, respectively. The cell uptake of this cluster is achieved in approximately 66 seconds, and the exerted magnetic force is measured to be 0.4 μN (Fig. 4). This force is one order on magnitude less than the interaction force that is measured in Fig. 6. Nevertheless, cell uptake of the cluster occurs immediately. *Please refer to the accompanying video that demonstrates the targeted penetration of the MCF-7 breast cancer cells using clusters of nanoparticles.*

The shape (aspect ratio of the cluster), size (affects the magnetic dipole and magnetic force), surface charge, and many other physicochemical factors [7] affect the cellular uptake and mechanism of internalization of nanoparticles. A recent report by Calero *et al.* has investigated the mechanism of internalization involved in super-paramagnetic iron-oxide nanoparticles (SPION) in MCF-7 cells [9]. It has been concluded that an active energy dependent transport mechanism is involved since it is only effective at 37°C and not 4°C. These results confirm several other studies reporting the

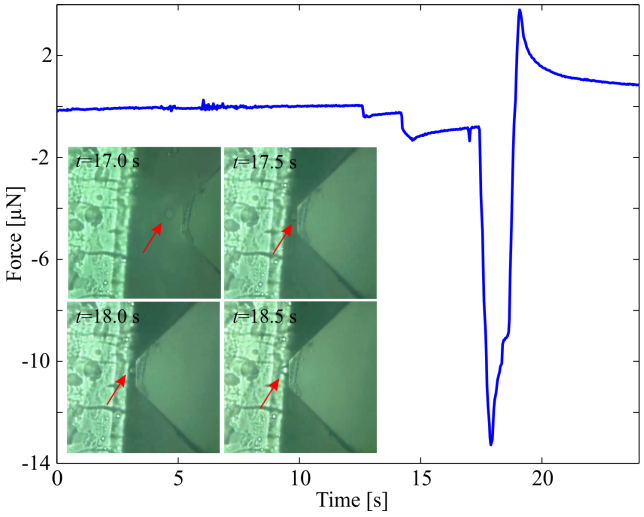

Fig. 6. Measuring the interaction force between an MCF-7 cell and the tip of a microforce sensing probe. The probe is moved towards the cell and a compression force is generated when the cell is in contact with the wall of the microfluidic channel. A compression force is measured with magnitude of 13.3 μN at time, t=17.5 seconds. The red arrow indicates the cell. This force does not cause permanent damage to the cell membrane and does not affect the morphology of the cell. *Please refer to the accompanying video that demonstrates the characterization of the MCF-7 cells using the microforce sensing probe.*

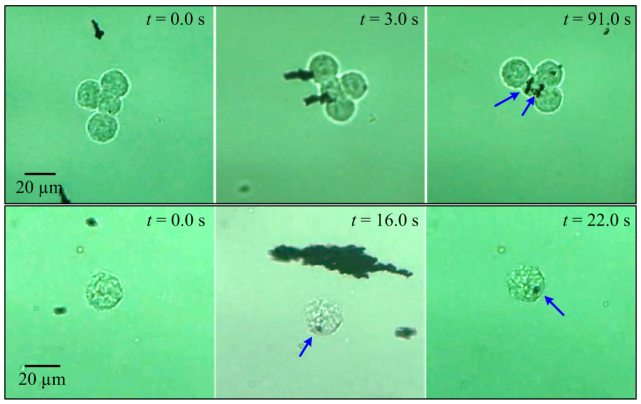

Fig. 7. Pre- and post-conditions of MCF-7 cell aggregate and single MCF-7 cell subjected to penetration using clusters of iron-oxide nanoparticles. Top: two clusters target cell aggregate and the uptake is observed after 91 seconds. Bottom: A cluster targets a cell and the uptake is achieved in 22 seconds. The applied magnetic field and gradient are 60 mT and 5 T.m^{-1}, respectively. The cell membrane is not damaged after the accumulation of the nanoparticles. *Please refer to the accompanying video that demonstrates the penetration of the cell under the influence of the controlled magnetic fields.*

ability of the cell to engulf the nanoparticles actively by endocytosis process. The specific type of endocytosis (e.g., phagocytosis, pinocytosis, macropinocytosis, clathrin mediated endocytosis, or caveolae-mediated endocytosis) of the nanoparticles depends on the type, size, and other properties of the nanoparticles. In an attempt to study the exact method of endocytosis occurring when MCF-7 cells are incubated with SPION, Calero *et al.* have preformed Transmission Electron Microscopy imaging of the MCF-7 cells. They have concluded that small aggregates (<200 nm) have been taken up by clathrin mediated endocytosis, whereas larger aggregates have been taken up by pinocytosis. Significant differences exist in the method of internalization in the cells according to the size of the nanoparticles. Our experimental results show that the endocytosis process can be accelerated by directing the nanoparticles towards the cells and achieve localization of these nanoparticles within the vicinity of the MCF-7 breast cancer cells.

IV. CONCLUSIONS AND FUTURE WORK

We achieve penetration of MCF-7 breast cancer cells using iron-oxide nanoparticles with a magnetic force less than 51 nN. The MCF-7 cells overcome interaction forces in excess of 13.3 μN. The cell uptake of the iron-oxide nanoparticles is accomplished under the influence of magnetic field gradient of 5 T.m^{-1} and magnetic field of 55.9 mT. The field and gradient are generated using an electromagnetic system with closed-configuration and motion control of the cluster of nanoparticles is done under microscopic guidance selectively towards the cells. Not only do we find that the nanoparticles uptake occurs immediately under magnetic field guidance, but we also observe that the targeted penetration does not cause damage or deformation to the cell membrane after the endocytosis process. In contrast to the conventional internalization methods that depend on incubation of cells and nanoparticles for long time, the magnetic-based cellular uptake is achieved immediately, and hence enables efficient *in vitro* experimentation in targeted therapy and nanomedicine.

As part of future studies, the iron-oxide nanoparticles will be coated with a chemotherapeutic agent and used in the penetration of the cancer cells. This study will be done in the presence of time-varying flow of a bodily fluid [21], [22]. The effect of the magnetic field on the accumulation and the uptake rate of the nanoparticles will be studied by taking Transmission Electron Microscopy images of the cells before and after the penetration. This study is essential to translate the experimental control of magnetic drug carriers and magnetic agents into *in vivo* experimentations. In addition, our electromagnetic system will be adapted to include an ultrasound imaging modality to provide feedback to the control system [23].

V. ACKNOWLEDGMENTS

The authors acknowledge the funding from the German University in Cairo and the DAAD-BMBF funding project.

The authors would like to thank Ms. Sherouk Mohamed for assistance with the fabrication of the iron-oxide nanoparticles. They would also like to thank Dr. Mohamed Serry for assistance with the Scanning Electron Microscopy imaging. Finally, they would also like to thank Prof. Khaled Abou Aisha for the guidance on the preparation of the MCF-7 breast cancer cells.

REFERENCES

[1] K. E. Peyer, L. Zhang, and B. J. Nelson, "Bio-inspired magnetic swimming microrobots for biomedical applications", *Nanoscale*, vol. 5, no. 4, pp. 1259-1272, November 2012.

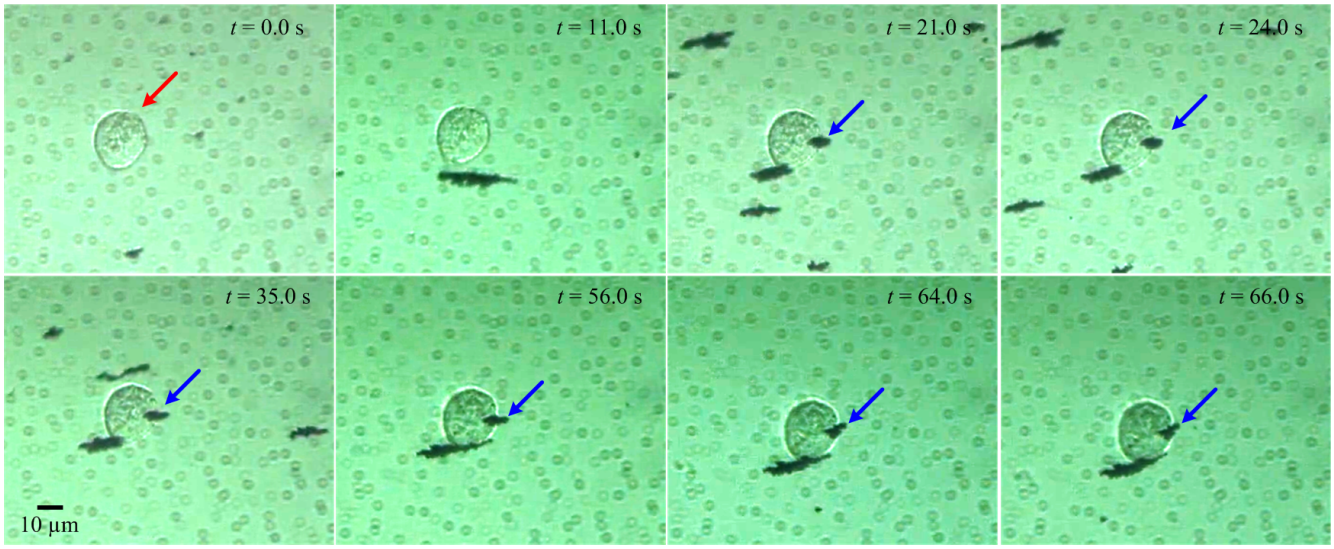

Fig. 8. Penetration of MCF-7 breast cancer cell (red arrow) using a cluster (blue arrow) of iron-oxide nanoparticles is achieved. The cluster is pulled towards the cell under the influence of the magnetic field gradient and penetration of the cell is achieved at time, t=21 seconds. The cluster of nanoparticles is partially engulfed by the cell at time, t=66 seconds. *Please refer to the accompanying video that demonstrates the penetration of the cell under the influence of the controlled magnetic fields.*

[2] S. Martel and M. Mohammadi, "Using a swarm of self-propelled natural microrobots in the form of flagellated bacteria to perform complex micro-assembly tasks," in *Proceedings of The IEEE International Conference on Robotics and Automation*, pp. 500-505, Alaska, USA, May 2010.

[3] C. Alexiou, W. Arnold, R. J. Klein, F. G. Parak, P. Hulin, C. Bergemann, W. Erhardt, S. Wagenpfeil, and A. S. Lübbe, "Locoregional cancer treatment with magnetic drug targeting," *Cancer Research*, vol. 60, pp. 6641-6648, December 2000.

[4] S. R. Rudge, T. L. Kurtz, C. R. Vessely, L. G. Catterall, and D. L. Williamson, "Preparation, characterization, and performance of magnetic iron-carbon composite microparticles for chemotherapy," *Biomaterials*, vol. 21, no. 14, pp. 1411–1420, July 1999.

[5] J. Wang and W. Gao, "Nano/Microscale Motors: Biomedical Opportunities and Challenges," *ACS Nano*, vol. 6, no. 7, pp. 5745-5751, July 2012.

[6] B. J. Nelson, I. K. Kaliakatsos, and J. J. Abbott, "Microrobots for minimally invasive medicine," *Annual Review of Biomedical Engineering*, vol. 12, pp. 55-85, April 2010.

[7] S. E. A. Gratton, P. A. Ropp, P. D. Pohlhaus, J. C. Luft, V. J. Madden, M. E. Napier, and J. M. DeSimone, "The effect of particle design on cellular internalization pathways," *Proceedings of National Academy of Science*, vol. 105, no. 33, pp. 11613–11618, August 2008.

[8] W. Wang, S. Li, L. Mair, S. Ahmed, T. J. Huang, and T. E. Mallouk, "Acoustic propulsion of nanorod motors inside living cells," *Angewandte Chemie*, vol. 126, no. 12, pp. 3265–3268, February 2014.

[9] M. Calero, M. Chiappi, A. Lazaro-Carrillo, M. J. Rodríguez, F. J. Chichón, K. Crosbie-Staunton, A. Prina-Mello, Y. Volkov, A. Villanueva and J. L. Carrascosa, "Characterization of interaction of magnetic nanoparticles with breast cancer cells," in *Journal of Nanobiotechnology*, vol. 13, no. 16, pp. 1–15, February 2015.

[10] S. Sanchez, A. A. Solovev, S. Schulze, and O. G. Schmidt, "Controlled manipulation of multiple cells using catalytic microbots," *Chemical Communications*, vol. 47, no. 2, pp. 698–700, January 2011.

[11] I. S. M. Khalil, V. Magdanz, S. Sanchez, O. G. Schmidt and S. Misra, "Magnetotactic bacteria and microjets: A comparative study," in *Proceedings of the IEEE/RSJ International Conference of Robotics and Systems (IROS)*, pp. 2035-2040, Tokyo, Japan, November 2013.

[12] J. Liu, V. Siragam, Z. Gong, J. Chen, C. Leung, Z. Lu, C.H. Ru, S.R. Xie, J. Luo, R. Hamilton, and Y. Sun, "Automated microrobotic characterization of cell-cell communication," in *Proceedings of the IEEE International Conference on Robotics and Automation (ICRA)*, pp. 469–474, Hong Kong, China, June 2014.

[13] E. T. Enikov and B. J. Nelson, "MEMS-based single-cell penetration force sensor," in *Proceedings of the SPIE 3834, Microrobotics and Microassembly*, pp. 40–46, August 1999.

[14] I. S. M. Khalil, V. Magdanz, S. Sanchez, O. G. Schmidt, L. Abelmann and S. Misra, "Magnetic control of potential microrobotic drug delivery systems: nanoparticles, magnetotactic bacteria and self-propelled microjets," in *Proceedings of the International Conference of the IEEE Engineering in Medicine and Biology Society (EMBC)*, pp. 5299-5302, Osaka, Japan, July 2013.

[15] T. H. Boyer, "The force on a magnetic dipole," *American Journal of Physics*, vol. 56, no. 8, pp. 688-692, August 1988.

[16] I. S. M. Khalil, R. M. P. Metz, B. A. Reefman, and S. Misra, "Magnetic-Based minimum input motion control of paramagnetic microparticles in three-dimensional space," *Proceedings of the IEEE/RSJ International Conference of Robotics and Systems (IROS)*, pp. 2053-2058, Tokyo, Japan, November 2013.

[17] I. S. M. Khalil, R. M. P. Metz, L. Abelmann, and S. Misra, "Interaction force estimation during manipulation of microparticles," in *Proceedings of the IEEE/RSJ International Conference of Robotics and Systems (IROS)*, pp. 950–956, Vilamoura, Algarve, Portugal, October 2012.

[18] I. S. M. Khalil, M. P. Pichel, L. Abelmann, and S. Misra, "Closed-loop control of magnetotactic bacteria," *The International Journal of Robotics Research*, vol. 32, no. 6, pp. 637-649, May 2013.

[19] M. P. Kummer, J. J. Abbott, B. E. Kartochvil, R. Borer, A. Sengul, and B. J. Nelson, "OctoMag: an electromagnetic system for 5-DOF wireless micromanipulation," *IEEE Transactions on Robotics*, vol. 26, no. 6, pp. 1006-1017, December 2010.

[20] I. S. M. Khalil, I. E. O. Gomaa, R. M. Abdel-Kader and S. Misra, "Magnetic-Based contact and non-contact manipulation of cell mock-ups and MCF-7 human breast cancer cells," *Smart Drug Delivery System*, Intech, ch. 9, pp. 219-235, February 2016.

[21] I. S. M. Khalil, V. Magdanz, S. Sanchez, O. G. Schmidt, and S. Misra, "The control of self-propelled microjets inside a microchannel with time-varying flow rates," *IEEE Transactions on Robotics*, vol. 30, no. 1, pp. 49-58, February 2014.

[22] I. S. M. Khalil, M. P. Pichel, O. S. Sukas, L. Abelmann, and S. Misra, "Control of magnetotactic bacterium in a micro-fabricated maze," in *Proceedings of the IEEE International Conference on Robotics and Automation (ICRA)*, pp. 5488-5493, Karlsruhe, Germany, May 2013.

[23] I. S. M. Khalil, P. Ferreira, R. Eleutério, C. L. de Korte, and S. Misra, "Magnetic-Based closed-loop control of paramagnetic microparticles using ultrasound feedback," in *Proceedings of the IEEE International Conference on Robotics and Automation (ICRA)*, Hong Kong, China, June 2014.